ICAS 2020 SHANG HAI
International Council of the Aeronautical Sciences
32nd Congress of the International Council of the Aeronautical Sciences
September 6-10, 2021
Pudong Shangri-La, Shanghai, China

DECENTRALIZED CONFLICT DETECTION AND RESOLUTION METHOD ACCOUNTING FOR UNCERTAINTIES OF TRAJECTORIES

Nobuhiro Yokoyama[1]

[1] National Defense Academy of Japan

Abstract

The present study proposes a new method for real-time decentralized conflict detection and resolution (CDR) for multiple aircraft under the assumption that four-dimensional trajectory-based operation is implemented. The proposed method in each aircraft simultaneously calculates the optimal ground speed vectors for all the involved aircraft while accounting for the uncertainty of the flight intent of neighboring aircraft and the actual wind condition. Because the uncertainty of the intent of the neighboring aircraft is discrete, we represent it with two ground speed vectors for neighboring aircraft as if each neighboring aircraft was adopting two trajectories, one representing direct travel to the planned waypoint and the other representing CDR in cooperation with the neighboring aircraft. At the same time, unnecessary multiplicities of the neighbor's intent are eliminated by monitoring the degree of conformance to the shared intent by inferring the actual intent in real time. Moreover, we take the uncertainty of the wind vector into account by its mean and covariance using quadratic functions of the ground speed vectors and incorporate them into the stochastic constraints on the airspeed limits. Through numerical simulations, the effectiveness of the proposed method was demonstrated.

Keywords: conflict detection and resolution, decentralized optimization, uncertainty, intent, wind condition

1. Introduction

One of the most important endeavors for the modernization of air traffic management is to replace conventional operations in highly structured airspace with trajectory-based operations (TBO). In TBO, strategic four-dimensional (4-D) trajectories [1] of individual aircraft with their own itineraries are planned, shared, and re-planned based on requests for and agreements on constraints on airspace capacity. Moreover, due to its potential usefulness in highly automated traffic management in congested airspace, 4-D TBO will also play an important role in operations of unmanned aerial system (UAS) traffic management and even its extension to the unified traffic management of multiple types of aircraft, such as UASs, electric vertical take-off and landing aircraft, and manned aircraft flying under visual flight rules. However, to improve operational flexibility and safety in tactical situations over relatively short time scales, it is crucial to allow trajectories to change according to the situation and delegate the responsibility for detecting and resolving conflict to individual aircraft. With this in mind, the objective of the present study is to develop a new method for real-time decentralized conflict detection and resolution (CDR) for multiple aircraft under implementation of 4-D TBO.

In general, decentralized CDR requires the prediction of future trajectories of neighboring aircraft [2] based on their current and past states and tactical flight intent [3-5], such as resolving conflict with neighboring aircraft in a cooperative way, directly traveling to the planned waypoint as scheduled, or skipping the planned waypoint to move on to the next waypoint. Such tactical flight intent can be shared in real time via data links. However, unlike the strategic 4-D trajectories, which can be changed according to negotiation among the involved stakeholders (e.g., pilots/operators of individual aircraft, dispatchers, and air traffic controllers), the tactical flight intent may change without notice in shorter time scales. Thus, it is possible that the actual intent may temporarily differ from the shared one. Furthermore, because the 4-D trajectories are premised on the time profiles of an aircraft's ground speed, it can be hard for an aircraft to track them due to their airspeed limits when

the actual wind conditions significantly differ from the predicted wind. Based on these viewpoints, the CDR method proposed herein accounts for the uncertainty of flight intent and actual wind condition.

A number of CDR methods accounting for uncertainty have been proposed [2, 4, 6-9], and these can roughly be categorized as worst-case methods and probabilistic methods. Worst-case methods compute extreme scenarios by generating a set of possible trajectories subject to uncertainty. Probabilistic methods also calculate a set of possible trajectories, but these sets include the associated probability density function of the uncertainty. If worst-case or probabilistic methods are applied to CDR, they can compute robustly safe trajectories compared to those not accounting for uncertainty. However, at the same time, they tend to result in overly conservative trajectories because each aircraft's feedback mechanism for the ground speed vector to fulfill its intent is not usually taken into account in uncertainty propagation. Moreover, if they are combined with decentralized optimizations that need to ensure that the resulting trajectories are compatible [9], the conservativeness can increase further.

Thus, to reduce the trajectory conservativeness in a decentralized optimization framework, the proposed method implemented in each aircraft simultaneously calculates the optimal ground speed vectors for all the involved aircraft under the assumption that each aircraft has a feedback mechanism to follow the optimized ground speed vector. While such a simultaneous optimization has previously been developed [10], the distinctive feature of the present method is the accommodation of uncertainty and a new optimization technique that is a variant of a reported method [11]. Because the uncertainty of the tactical intent of the neighboring aircraft is discrete, we represent it by two ground speed vectors for neighboring aircraft, as if each neighboring aircraft was adopting two trajectories, one representing direct travel to the planned 4-D waypoint and the other representing the conflict resolution in cooperation with neighboring aircraft. In addition, to reduce the conservativeness further, unnecessary multiplicities of the neighbor's intent are eliminated by monitoring the degree of conformance to the shared intent by inferring the actual intent in real time. For this inference, we apply a modified version of the method developed in previous studies [5, 11]. Moreover, we take the uncertainty of the wind vector into account by its mean and covariance using quadratic functions of the ground speed vectors and incorporate them into the stochastic constraints on the airspeed limits. Although the size of the optimization problem in each aircraft is quadratic with respect to the number of involved aircraft, it is small enough for real-time applications because it is formulated as a simple decision-making problem described by a relatively small quadratically constrained quadratic program (QCQP). The non-convexities in the resulting QCQP are handled by a convexification technique in which the non-convex constraints, involving the mean and covariance of the wind uncertainty, are aggregated as a single concave constraint and sequentially linearized. Thus, the optimization problem here is sequentially solved via a second-order cone program (SOCP) [12], which can be performed in real time by commercially available off-the-shelf software.

Through numerical simulations, the effectiveness of the proposed method was confirmed in terms of its robustness and the reduced conservativeness of the calculated trajectories under the uncertainties of flight intent and wind conditions.

2. Proposed method for conflict detection and resolution

2.1 Model of Aircraft Motion

For simplicity, we assume that the motion of an aircraft is constrained to the horizontal plane. The state equations for the aircraft are written as follows:

$$\begin{bmatrix} \dot{x} \\ \dot{y} \\ \dot{V} \\ \dot{\psi} \end{bmatrix} = \begin{bmatrix} V\cos\psi + w_x \\ V\sin\psi + w_y \\ a \\ (g\tan\phi + \dot{w}_x\sin\psi - \dot{w}_y\cos\psi)/V \end{bmatrix}, \tag{1}$$

where (x, y) is the position of the aircraft in the horizontal coordinate system, V is the airspeed, ψ is the heading angle, w_x and w_y are respectively the x and y components of the wind velocity, g is gravitational acceleration, ϕ is the bank angle, and a is the airspeed acceleration.

Let u_a, v_a and u, v be x and y components of the airspeed and the ground speed, respectively:

$$u_a := V\cos\psi, \quad v_a := V\sin\psi, \quad u := u_a + w_x, \quad v := v_a + w_y . \tag{2}$$

Then, we can rewrite Eq. (1) as

$$\begin{bmatrix} \dot{x} \\ \dot{y} \\ \dot{u} \\ \dot{v} \end{bmatrix} = \begin{bmatrix} u \\ v \\ \{a/V + (\dot{w}_x u_a + \dot{w}_y v_a)/V^2\}u_a - (g\tan\phi/V)v_a \\ \{a/V + (\dot{w}_x u_a + \dot{w}_y v_a)/V^2\}v_a + (g\tan\phi/V)u_a \end{bmatrix} . \tag{3}$$

In practice, a depends on other variables, such as $V, \dot{w}_x, \dot{w}_y, \psi$, and ϕ, and we assume that its value can be directly controlled by a low-level controller. Thus, by regarding $[x \;\; y \;\; u \;\; v]^T$ and $[a \;\; \phi]^T$ as the state and the control input, respectively, we adopt Eq. (3) as the state equation for each aircraft.

2.2 Overview of the Proposed Method

Let us consider the decentralized CDR of multiple aircraft that yields the dynamic model above at every sampling time $t = k\Delta t \;\; (k = 0,1,\cdots)$. Hereafter, M denotes the number of involved aircraft, the subscript k denotes the time index corresponding to $t = k\Delta t$, and the superscript (i) denotes the index for the i-th aircraft, where $i \in \{1,\cdots,M\}$. Let $a_n^{(i)}, b_n^{(i)}$, and $T_n^{(i)}$ respectively denote the x-position, y-position, and scheduled transit time for the n-th waypoint of aircraft i. Furthermore, we make the following assumptions:

- The strategic flight plan for each aircraft $i \in \{1,\cdots,M\}$ is represented as a set of $L^{(i)}$ waypoints, that is, $\{(a_n^{(i)}, b_n^{(i)}, T_n^{(i)}),\ n = 1,\cdots,L^{(i)}\}$, and this plan is shared with all the involved aircraft. Also, the lower and upper limits of the airspeed of each aircraft i, denoted by $V_{\min}^{(i)}$ and $V_{\max}^{(i)}$, respectively, are also shared with all the involved aircraft.
- The position and ground speed vector for each aircraft $i \in \{1,\cdots,M\}$ at each sampling time $(k = 0,1,\cdots)$, that is, $[x_k^{(i)} \;\; y_k^{(i)}]^T$ and $[u_k^{(i)} \;\; v_k^{(i)}]^T$, are shared with all the involved aircraft in real time. In addition, it is possible to observe or estimate $[w_{xk}^{(i)} \;\; w_{yk}^{(i)}]^T$, and thus $[u_{ak}^{(i)} \;\; v_{ak}^{(i)}]^T$, in real time, but there is some uncertainty (i.e., error) in these observations or estimates.
- The tactical flight intent for each aircraft is shared via data link in real time, although inconsistency with the actual intent is possible. For simplicity, the tactical flight intent is either going directly to the planned 4-D waypoint (referred to as WP intent), or performing CDR with the neighboring aircraft in a cooperative way (referred to as CDR intent).

Although it is possible to extend the proposed method to be applicable to cases where the number of neighboring aircraft is different for individual aircraft, we adopt the above assumptions for simplicity. Figure 1 depicts an input/output flowchart for each sampling time $t = k\Delta t \;\; (k = 0,1,\cdots)$ in the proposed method. Given the trajectories observed in real time, each aircraft infers the actual intent of each neighboring aircraft and monitors its conformance to the shared one. If the degree of conformance (to be defined later) is sufficient, then the inferred intent is considered “validated” and entered alone into the optimization process. Otherwise, both the WP intent and the CDR intent are considered “possible,” and both are entered into the optimization process. In the optimization process, each aircraft simultaneously calculates the optimal ground speed vectors for all the involved aircraft by minimizing their deviation from the strategic flight plans under the constraints for conflict resolution based on the entered (either single or dual) intent of individual aircraft. The wind uncertainty is also considered in the procedure. After calculating its own optimal ground speed vector, each aircraft follows this vector as much as possible with feedback control. The problems solved at each stage of the method are detailed in the following subsections.

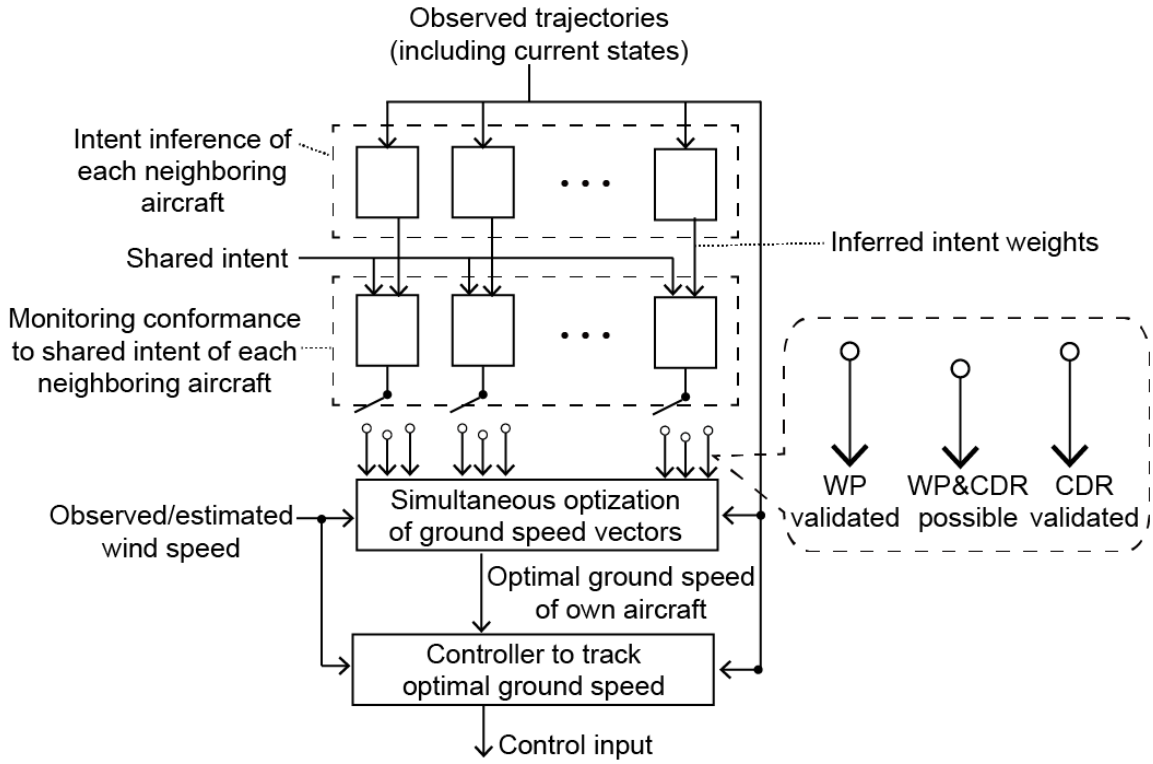

Figure 1 – Input/output flowchart of the proposed method.

2.3 Inference and Conformance Monitoring of Intent

The intent inference method adopted here solves the inverse optimal control problem [5], that is, it calculates the weight of each term of the objective function that best explains the tactical flight intent behind an observed trajectory. By incorporating the second-order optimality condition, specifically the positive definiteness of the projected Hessian of the Lagrangian [13], the method accounts for both the necessity and sufficiency of the approximate local optimality of the given trajectory.

Let $q_{n|k}^{(i)}$ be the weight corresponding to the i-th aircraft's intent to go directly to the n-th waypoint. Similarly, let $s_{l|k}^{+(i)}$ and $s_{l|k}^{-(i)}$ be the weights to resolve conflict with the l-th aircraft by making a right or left turn, respectively. These weights are assumed to be nonnegative and are normalized by

$$\sum_{n=1}^{L^{(i)}} q_{n|k}^{(i)} + \sum_{l=1}^{M} (s_{l|k}^{+(i)} + s_{l|k}^{-(i)}) = 1 . \tag{4}$$

In the present study, we apply a modified version of the inference method developed in the previous study [11]. The modifications were made to introduce binary variables $\alpha_{n|k}^{(i)} \in \{0,1\}$ to represent the uniqueness of the objective waypoint:

$$0 \le q_{n|k}^{(i)} \le \alpha_{n|k}^{(i)}, \quad n = 1, \cdots, L^{(i)} \tag{5}$$

$$\sum_{n=1}^{L^{(i)}} \alpha_{n|k}^{(i)} = 1 . \tag{6}$$

Moreover, we also introduced additional binary variables $\beta_{l|k}^{(i)} \in \{0,1\}$ to represent the alternative nature of turning right or left in the intent of conflict resolution:

$$\left.\begin{aligned} s_{l|k}^{+(i)} &\le \beta_{l|k}^{(i)} \\ s_{l|k}^{-(i)} &\le 1 - \beta_{l|k}^{(i)} \end{aligned}\right\}, \quad l = 1, \cdots, M, (l \ne i) \tag{7}$$

Thus, the resulting inverse optimal control problem becomes a mixed-integer quadratic programming problem. Details of the method except for the modification above have previously been reported [11]. It should be noted that the intent inference in the proposed method is performed based on the trajectories of the ground speed vectors rather than those of the airspeed vectors. This is because not only the flight intent modelled in the present study is based on the ground speed vectors, but also the airspeed vectors can be sensitive to the wind uncertainty.

The inferred intent is thus quantified by the weights defined above and used for the subsequent conformance monitoring, that is, we monitor their time profiles to check the conformance of the inferred intent to the shared intent in the following manner:

- If the shared intent of the i-th aircraft is WP and Eq. (8) below holds for a consecutive sequence of sampling times $m = k-k_1,\cdots,k-1,k$ under given k_1 and ε_1, then the WP intent and the CDR intent of the i-th aircraft are considered "validated" and "inactive," respectively.

$$\sum_{n=1}^{L^{(i)}} q_{n|m}^{(i)} \geq \varepsilon_1 \tag{8}$$

- If the shared intent of the i-th aircraft is CDR, and Eq. (9) holds for a consecutive sequence of sampling times $m = k-k_2,\cdots,k-1,k$ under given k_2 and ε_2, then the WP intent and the CDR intent of the i-th aircraft are considered "inactive" and "validated," respectively.

$$\sum_{l=1}^{M} (s_{l|m}^{+(i)} + s_{l|m}^{-(i)}) \geq \varepsilon_2 \tag{9}$$

- If none of the above conditions hold, both the CDR and WP intent of the i-th aircraft are considered "possible."

In addition, for each aircraft i, we assign an integer variable $r_k^{(i)}$ by setting $r_k^{(i)} = 1$ if its CDR intent is validated, $r_k^{(i)} = 0$ if its CDR and WP intent are possible, and $r_k^{(i)} = -1$ if its WP intent is validated.

2.4 Process to Optimize Ground Speed Vectors

In this process, a set of optimal ground speed vectors at current time $t = k\Delta t$ are calculated to reflect the validated or possible intent of each neighboring aircraft. Let us define the following sets of aircraft indices as $I := \{1,\cdots,M\}$, $Q_k := \{i \mid r_k^{(i)} \in \{-1,0\}\}$, $Q_k^+ = \{i \mid r_k^{(i)} = -1\}$, $S_k := \{i \mid r_k^{(i)} \in \{0,1\}\}$, and $S_k^+ := \{i \mid r_k^{(i)} = 1\}$. By definition, $Q_k \cap S_k^+ = S_k \cap Q_k^+ = I$. In addition, for any $i \in S_k^+$, let us modify $q_{n|k}^{(i)}$ to 1, where n corresponds to the currently intended waypoint according to the strategic flight plan, and let $[x_k^{(i)} \;\; y_k^{(i)}]^T$ and $[u_k^{(i)} \;\; v_k^{(i)}]^T$ denote the current position and ground speed vector, respectively.

Then, at the first stage, each aircraft solves the following problem to calculate the ideal ground speed vectors for all $i \in Q_k$ to reach its individual waypoint starting from its current position:

$$\underset{u^{(i)},v^{(i)},\forall i \in Q_k}{\text{minimize}}$$

$$J_1 := \sum_{i \in Q_k} \sum_{n=1}^{L^{(i)}} q_{n|k}^{(i)} \left\| \begin{bmatrix} u^{(i)} \\ v^{(i)} \end{bmatrix} - \frac{1}{T_n^{(i)} - k\Delta t} \begin{bmatrix} a_n^{(i)} - x_k^{(i)} \\ b_n^{(i)} - y_k^{(i)} \end{bmatrix} \right\|^2 \tag{10}$$

subject to

$$(V_{\min}^{(i)})^2 \leq (u^{(i)} - w_{xk}^{(i)})^2 + (v^{(i)} - w_{yk}^{(i)})^2 \leq (V_{\max}^{(i)})^2, \quad \forall i \in Q_k . \tag{11}$$

It should be noted that only one of the weights $q_{1|k}^{(i)},\cdots,q_{L^{(i)}|k}^{(i)}$ equals 1, and the remaining weights are zero. Thus, without Eq. (11), which denotes the constraints on the airspeed limits, the solution of the minimization of Eq. (10) would attain an accurate transit to the n-th waypoint corresponding to $q_{n|k}^{(i)} = 1$ at the scheduled time. In practice, the problem above can be solved individually for each $i \in Q_k$, but for the sake of notational simplicity, we formulate it in an aggregated way.

Let $\overline{u}_k^{(i)}, \overline{v}_k^{(i)}$ $\forall i \in Q_k$ be the solutions to the problem above. Then, at the second stage, each aircraft calculates the optimal ground speed vectors for all aircraft reflecting their "validated" and "possible" intent by solving the following problem:

$$\underset{u^{(i)},v^{(i)},\forall i \in I}{\text{minimize}}$$

$$J_2 := \sum_{i \in S_k} \left[\sum_{n=1}^{L^{(i)}} q_{n|k}^{(i)} \left\| \begin{bmatrix} u^{(i)} \\ v^{(i)} \end{bmatrix} - \frac{1}{T_n^{(i)} - k\Delta t} \begin{bmatrix} a_n^{(i)} - x_k^{(i)} \\ b_n^{(i)} - y_k^{(i)} \end{bmatrix} \right\|^2 + \mu \left\| \begin{bmatrix} u^{(i)} - u_{\text{prev}}^{(i)} \\ v^{(i)} - v_{\text{prev}}^{(i)} \end{bmatrix} \right\|^2 \right] \tag{12}$$

subject to

$$(V_{\min}^{(i)})^2 \le (u^{(i)} - w_{xk}^{(i)})^2 + (v^{(i)} - w_{yk}^{(i)})^2 \le (V_{\max}^{(i)})^2, \ \forall i \in S_k \tag{13}$$

$$(\boldsymbol{n}_k^{(i,l)})^T \begin{bmatrix} u^{(i)} - u^{(l)} \\ v^{(i)} - v^{(l)} \end{bmatrix} \ge 0, \quad \forall i \in S_k, \ \forall l \in S_k \cap \{i+1, \cdots, M\} \tag{14}$$

$$(\boldsymbol{n}_k^{(i,l)})^T \begin{bmatrix} u^{(i)} - \overline{u}_k^{(l)} \\ v^{(i)} - \overline{v}_k^{(l)} \end{bmatrix} \ge 0, \quad \forall i \in S_k, \ \forall l \in Q_k \tag{15}$$

$$\begin{bmatrix} u^{(i)} \\ v^{(i)} \end{bmatrix} = \begin{bmatrix} \overline{u}_k^{(i)} \\ \overline{v}_k^{(i)} \end{bmatrix}, \quad \forall i \in Q_k^+ \tag{16}$$

where μ is a positive parameter, $[u_{prev}^{(i)} \ \ v_{prev}^{(i)}]^T$ is a solution calculated at the previous sampling time $t = (k-1)\Delta t$, and

$$\boldsymbol{n}_k^{(i,l)} = \begin{cases} \boldsymbol{x}_k^{(i,l)} - [(\boldsymbol{x}_k^{(i,l)})^T \boldsymbol{e}_k^{(i,l)+}]\boldsymbol{e}_k^{(i,l)+} & : \text{if } \| \boldsymbol{d}_k^{(i,l)+} \| \le \| \boldsymbol{d}_k^{(i,l)-} \| \\ \boldsymbol{x}_k^{(i,l)} - [(\boldsymbol{x}_k^{(i,l)})^T \boldsymbol{e}_k^{(i,l)-}]\boldsymbol{e}_k^{(i,l)-} & : \text{otherwise} \end{cases}$$

$$\boldsymbol{e}_k^{(i,l)+} := \begin{bmatrix} \sqrt{1-(\delta_k^{(i,l)})^2} & -\delta_k^{(i,l)} \\ \delta_k^{(i,l)} & \sqrt{1-(\delta_k^{(i,l)})^2} \end{bmatrix} \frac{(-\boldsymbol{x}_k^{(i,l)})}{\| \boldsymbol{x}_k^{(i,l)} \|}, \quad \boldsymbol{e}_k^{(i,l)-} := \begin{bmatrix} \sqrt{1-(\delta_k^{(i,l)})^2} & \delta_k^{(i,l)} \\ -\delta_k^{(i,l)} & \sqrt{1-(\delta_k^{(i,l)})^2} \end{bmatrix} \frac{(-\boldsymbol{x}_k^{(i,l)})}{\| \boldsymbol{x}_k^{(i,l)} \|},$$

$$\boldsymbol{x}_k^{(i,l)} := \begin{bmatrix} x_k^{(i)} - x_k^{(l)} \\ y_k^{(i)} - y_k^{(l)} \end{bmatrix}, \quad \delta_k^{(i,l)} := \min\left(1, \frac{R}{\| \boldsymbol{x}_k^{(i,l)} \|}\right)$$

$$\boldsymbol{d}_k^{(i,l)+} := [\boldsymbol{I} - \boldsymbol{e}_k^{(i,l)+}(\boldsymbol{e}_k^{(i,l)+})^T] \begin{bmatrix} u_k^{(i)} - u_k^{(l)} \\ v_k^{(i)} - v_k^{(l)} \end{bmatrix}, \quad \boldsymbol{d}_k^{(i,l)-} := [\boldsymbol{I} - \boldsymbol{e}_k^{(i,l)-}(\boldsymbol{e}_k^{(i,l)-})^T] \begin{bmatrix} u_k^{(i)} - u_k^{(l)} \\ v_k^{(i)} - v_k^{(l)} \end{bmatrix},$$

where R is the required minimum aircraft separation. Figure 2 depicts the conflict cone between two aircraft and some of the relevant variables given above. It should be noted that $\boldsymbol{n}_k^{(i,l)}$ corresponds to the vector normal to the conflict cone's boundary that is closer to the current relative speed vector $[u_k^{(i)} - u_k^{(l)} \ \ v_k^{(i)} - v_k^{(l)}]^T$. Thus, Eqs. (14) and (15) mean that the relative speed vector should be optimized to be outside of the boundary of the conflict cone.

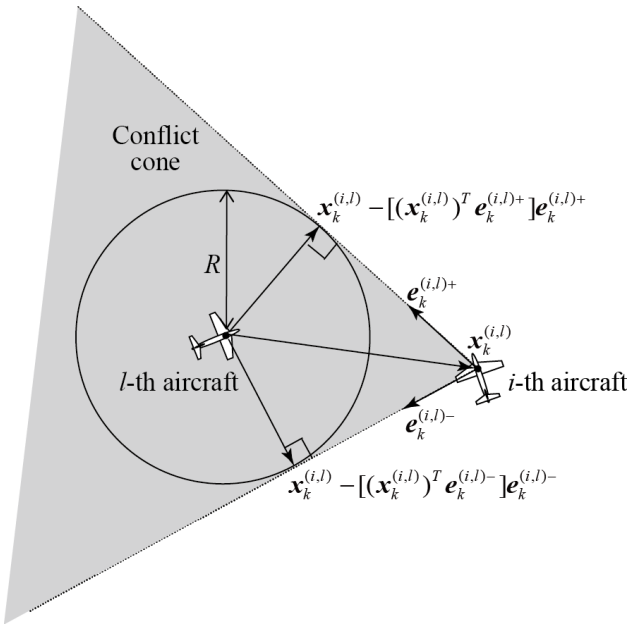

Figure 2 – Conflict cone and relevant variables.

Equation (14) denotes the constraints on the cooperative conflict resolutions between any pair of aircraft having the "validated" or "possible" CDR intent. Conversely, Eq. (15) denotes constraints on the unilateral conflict resolutions by any of the aircraft having the "validated" or "possible" CDR intent with any of that having "validated" or "possible" WP intent. (Note that the latter aircraft are presumed

to go directly to the planned waypoint based on the solution of the first optimization problem.) Thus, if the l-th aircraft has a "possible" intent for both WP and CDR, twofold conflict resolution constraints, specifically Eqs. (14) and (15), are enforced to represent the discrete uncertainty of the l-th aircraft's intent. In contrast, if the l-th aircraft's intent is "validated," then the uncertainty is eliminated to reduce unnecessary conservativeness.

It should be noted that Eqs. (11) and (13) involve the wind speed vector $[w_{xk}^{(i)} \;\; w_{yk}^{(i)}]^T$, which has the uncertainty expressed by the assumption given in 2.2. To express this assumption mathematically, we define the stochastic model of the wind speed as follows:

$$\begin{aligned} w_x(t,x,y) &= \hat{w}_x(t,x,y) + \sum_{j=1}^{N} g_j(t,x,y) z_j \\ w_y(t,x,y) &= \hat{w}_y(t,x,y) + \sum_{j=1}^{N} g_j(t,x,y) z_{j+N} \end{aligned}, \tag{17}$$

where N is a positive integer, $\hat{w}_x$ and $\hat{w}_y$ are the means, $g_1,\cdots,g_N$ characterize the spatial and temporal correlations of wind velocities, and $z_1,\cdots,z_{2N}$ are stochastic variables independently following the normal distribution $\mathcal{N}(0,1)$. Substituting Eq. (17) into the squared airspeed gives

$$\begin{aligned} &[u - w_x(t,x,y)]^2 + [v - w_y(t,x,y)]^2 \\ &= \left[u - \hat{w}_x(t,x,y) - \sum_{j=1}^{N} g_j(t,x,y) z_j \right]^2 + \left[v - \hat{w}_y(t,x,y) - \sum_{j=1}^{N} g_j(t,x,y) z_{j+N} \right]^2, \\ &= [u - \hat{w}_x(t,x,y)]^2 + [v - \hat{w}_y(x,y)]^2 + h(t,x,y,u,v,z) \end{aligned} \tag{18}$$

where $z := [z_1 \cdots z_{2N}]^T$ and $h(x,y,u,v,z)$ constitute a stochastic term defined by

$$\begin{aligned} h(x,y,u,v,z) := &\left[\sum_{j=1}^{N} g_j(t,x,y) z_j \right]^2 - 2[u - \hat{w}_x(t,x,y)] \sum_{j=1}^{N} g_j(t,x,y) z_j \\ &+ \left[\sum_{j=1}^{N} g_j(t,x,y) z_{j+N} \right]^2 - 2[u - \hat{w}_x(t,x,y)] \sum_{j=1}^{N} g_j(t,x,y) z_{j+N} \end{aligned}. \tag{19}$$

The term $h(x,y,u,v,z)$ is quadratic with respect to the stochastic variables $z_1,\cdots,z_{2N}$ that independently follow $\mathcal{N}(0,1)$. Its mean $\hat{h}$ and variance $\hat{\sigma}^2$ are given by the following analytical expressions:

$$\hat{h}(t,x,y) := \mathbb{E}[h(t,x,y,u,v,z)] = 2\sum_{j=1}^{N} g_j^2(t,x,y), \tag{20}$$

$$\begin{aligned} \hat{\sigma}^2(t,x,y,u,v) &:= \mathbb{E}[\{h(t,x,y,u,v,z) - \hat{h}(t,x,y)\}^2] \\ &= 6\sum_{j=1}^{N} g_j^4(t,x,y) - \hat{h}^2(t,x,y) + 2[\{u - \hat{w}_x(t,x,y)\}^2 + \{v - \hat{w}_y(t,x,y)\}^2]\hat{h}(t,x,y) \end{aligned}, \tag{21}$$

where we used $\mathbb{E}(z_j) = \mathbb{E}(z_j{}^3) = 0, \mathbb{E}(z_j{}^2) = 1$ and $\mathbb{E}(z_j{}^4) = 3$. From Eqs. (20) and (21), if $t,x,$ and y are given, the mean $\hat{h}$ is the constant and $\hat{\sigma}^2$ is the quadratic function of u and v. Thus, by using these equations, we convert Eqs. (11) and (13), respectively, to

$$\left.\begin{aligned} (V_{\min}^{(i)})^2 + \gamma\sigma^{(i)} \le (u^{(i)} - \hat{w}_{xk}^{(i)})^2 + (v^{(i)} - \hat{w}_{yk}^{(i)})^2 + \hat{h}_k^{(i)} \le (V_{\max}^{(i)})^2 - \gamma\sigma^{(i)} \\ (\sigma^{(i)})^2 = \hat{\sigma}^2(k\Delta t, x_k^{(i)}, y_k^{(i)}, u^{(i)}, v^{(i)}) \end{aligned}\right\}, \; \forall i \in Q_k \tag{22}$$

and

$$\left.\begin{aligned} (V_{\min}^{(i)})^2 + \gamma\sigma^{(i)} \le (u^{(i)} - \hat{w}_{xk}^{(i)})^2 + (v^{(i)} - \hat{w}_{yk}^{(i)})^2 + \hat{h}_k^{(i)} \le (V_{\max}^{(i)})^2 - \gamma\sigma^{(i)} \\ (\sigma^{(i)})^2 = \hat{\sigma}^2(k\Delta t, x_k^{(i)}, y_k^{(i)}, u^{(i)}, v^{(i)}) \end{aligned}\right\}, \; \forall i \in S_k \tag{23}$$

where $\hat{w}_{xk}^{(i)}$, $\hat{w}_{yk}^{(i)}$, and $\hat{h}_k^{(i)}$ denote $\hat{w}_x(k\Delta t, x_k^{(i)}, y_k^{(i)})$, $\hat{w}_y(k\Delta t, x_k^{(i)}, y_k^{(i)})$, and $\hat{h}(k\Delta t, x_k^{(i)}, y_k^{(i)})$, respectively; $\sigma_k^{(i)}$ is an additional variable representing the standard deviation; and γ is a constant coefficient that multiplies the standard deviation for tuning the potential for constraint violation. Thus, the two-stage optimization problems are converted as follows:

- First problem: minimize Eq. (10) subject to Eq. (22).
- Second problem: minimize Eq. (12) subject to Eqs. (14)-(16) and (23).

Because these problems are non-convex QCQPs, they belong to the class of NP-hard problems. To solve these efficiently, the proposed method transforms each problem to minimize a convex objective function subject to multiple convex constraints and a single concave constraint in the following way. The non-convexities exist only in Eqs. (22) and (23) for the first and second problems, respectively. Thus, we aggregate the non-convexity in these equations to a single concave constraint. For brevity, we focus only on the second problem and note that the first problem can also be solved in the same way. By introducing an additional variable $\lambda^{(i)}$, which corresponds to the squared airspeed, Eq. (23) can be rewritten as

$$(u^{(i)} - \hat{w}_{xk}^{(i)})^2 + (v^{(i)} - \hat{w}_{yk}^{(i)})^2 \geq \lambda^{(i)}, \ \forall i \in S_k \tag{24}$$

$$(u^{(i)} - \hat{w}_{xk}^{(i)})^2 + (v^{(i)} - \hat{w}_{yk}^{(i)})^2 \leq \lambda^{(i)}, \ \forall i \in S_k \tag{25}$$

$$(V_{\min}^{(i)})^2 + \gamma\sigma^{(i)} \leq \lambda^{(i)} + \hat{h}_k^{(i)} \leq (V_{\max}^{(i)})^2 - \gamma\sigma^{(i)}, \ \forall i \in S_k \tag{26}$$

$$(\sigma^{(i)})^2 \leq 6\sum_{j=1}^{N} (g_{jk}^{(i)})^4 - (\hat{h}_k^{(i)})^2 + 2\hat{h}_k^{(i)}\lambda^{(i)}, \ \forall i \in S_k \tag{27}$$

$$(\sigma^{(i)})^2 \geq \hat{\sigma}^2(k\Delta t, x_k^{(i)}, y_k^{(i)}, u^{(i)}, v^{(i)}), \ \forall i \in S_k \tag{28}$$

where $g_{jk}^{(i)} := g_j^{(i)}(k\Delta t, x_k^{(i)}, y_k^{(i)})$. In these inequalities, only Eq. (24) is concave, while the remaining inequalities, including Eq. (28), which is a second-order cone, are convex. Under the constraints of Eq. (25), Eq. (24) can further be rewritten as the following aggregated equation:

$$\sum_{i \in S_k} [(u^{(i)} - \hat{w}_{xk}^{(i)})^2 + (v^{(i)} - \hat{w}_{yk}^{(i)})^2 - \lambda^{(i)}] \geq 0 . \tag{29}$$

Thus, the set constrained by Eq. (23) is equivalently converted to the set constrained by the multiple convex constraints of Eqs. (25)-(28) and the single concave constraint of Eq. (29).

To handle the non-convexity in Eq. (29), we linearize Eq. (29) around the given references $[u_r^{(i)} \ \ v_r^{(i)}]^T, i \in S_k$ in the following way:

$$\left.\begin{aligned} &\sum_{i \in S_k} [2\{(u_r^{(i)} - \hat{w}_{xk}^{(i)})(u^{(i)} - u_r^{(i)}) + (v_r^{(i)} - \hat{w}_{yk}^{(i)})(v - v_r^{(i)})\} + (u_r^{(i)} - \hat{w}_{xk}^{(i)})^2 + (v_r^{(i)} - \hat{w}_{yk}^{(i)})^2 - \lambda^{(i)}] + \zeta \geq 0 \\ &\zeta \geq 0 \end{aligned}\right\}, \tag{30}$$

where ζ is a slack variable. In addition, we augment the objective function with a penalty term for non-zero ζ as follows:

$$J_2 + \rho\zeta , \tag{31}$$

where ρ is a nonnegative parameter. We iteratively solve the problem to minimize Eq. (31) subject to Eqs. (14)-(16), (25)-(28), and (30) by updating the references $[u_r^{(i)} \ \ v_r^{(i)}]^T, i \in S_k$ with the obtained solution. If a feasible solution to the problem with $\zeta = 0$ is found, this indicates that the solution is also feasible for the original non-convex problem, because, due to the concavity of Eq. (29), the solution satisfying Eq. (30) with $\zeta = 0$ also satisfies Eq. (29). We increase the magnitude of ρ as the iteration progresses so that ζ converges to zero whenever possible.

As an initial reference required at each sampling time $t = k\Delta t$, we use the solution obtained at the previous sampling time $t = (k-1)\Delta t$ if available; otherwise, we use the current ground speed vectors. The convexification technique adopted here is a variant of the previously developed method [11], where a modification was made to accommodate the standard deviation of the wind speed. Unlike the alternating direction of multipliers method [14], which is also a popular approach to solve non-convex QCQPs, the approach here has the advantage of not requiring adjoint variables whose physical meanings and appropriate guesses are generally not available. The resulting formulation above is a type of difference of convex (DC) programming problem [15], and the penalty approach adopted above is similar to the penalty convex-concave approach [16]. The distinctive feature of our approach here is the preservation of the sparse structure of the quadratic polynomials with respect to each i by introducing the additional variable $\lambda^{(i)}$. Thus, the convexified problems to be solved

sequentially become sparse SOCPs, which can be efficiently solved via commercially available off-the-shelf software. While the sizes of the first and second optimization problems are respectively linear and quadratic with respect to the number of aircraft M, the computational time to solve these with a moderate size of M is manageable due to the sparsity stated above and the fact that the only decision variables are the ones at $t = k\Delta t$.

2.5 Controller to Follow the Optimized Ground Speed

The proposed method involves a controller for each aircraft to follow the calculated ground speed vector as closely as possible under wind uncertainty.

For the sake of notational simplicity, we omit the superscript (i) here. The control inputs for Eq. (3), a and ϕ, are calculated by the following simple control law:

$$\begin{bmatrix} a \\ g\tan\phi \end{bmatrix} = \frac{1}{\tau\hat{V}}\begin{bmatrix} \hat{u}-\hat{w}_x & \hat{v}-\hat{w}_y \\ -\hat{v}+\hat{w}_y & \hat{u}-\hat{w}_x \end{bmatrix}\begin{bmatrix} u^*-\hat{u} \\ v^*-\hat{v} \end{bmatrix} - \frac{1}{\hat{V}}\begin{bmatrix} (d\hat{w}_x/dt)(\hat{u}-\hat{w}_x)+(d\hat{w}_x/dt)(\hat{v}-\hat{w}_y) \\ 0 \end{bmatrix}, \tag{32}$$

where u^* and v^* denote the optimal ground speed vector calculated by each aircraft for itself by the process in 2.4; $\hat{u}$, $\hat{v}$, and $\hat{V}$ are observed or estimated values of u, v, and V, respectively; and τ is a tuning parameter corresponding to the time constant. If all the observed or estimated values are the same as the actual values, substituting Eq. (32) for the third and fourth rows of Eq. (3) yields the following first-order lag system of the ground speed vector:

$$\begin{bmatrix} \dot{u} \\ \dot{v} \end{bmatrix} = \frac{1}{\tau}\left(\begin{bmatrix} u^* \\ v^* \end{bmatrix} - \begin{bmatrix} u \\ v \end{bmatrix}\right). \tag{33}$$

In practice, a more sophisticated controller to robustly compensate for future wind uncertainty, such as the stochastic model predictive controller [17], can be applied. Nevertheless, we adopted the controller above to simply evaluate the effectiveness of the process in 2.3 and 2.4 in the simulation study.

3. Numerical Examples

We performed numerical simulations to confirm the effectiveness of the proposed method. Here, we considered the traffic management of homogeneous UASs. The parameters used in the simulations are summarized in Table 1, where “inference steps” means the number of time steps of the latest trajectory required for the intent inference. Although elaborate functions can be adopted as the functions in the wind speed model in Eq. (17), they were simply assumed as follows:

$$\begin{aligned} &\hat{w}_x = c\cdot x \ \text{m/s}, \quad c = 1.0\times10^{-4} \ 1/\text{s}, \quad \hat{w}_y = 5.0 \ \text{m/s}, \\ &N = 1, \quad g_1 = 2.0 \ \text{m/s} \end{aligned} \tag{34}$$

First, we considered CDR among three aircraft under the following two cases:

- Case A – All aircraft have the CDR intent and share them throughout the simulation.
- Case B – Only the third aircraft $(i = 3)$ has the WP intent and the remaining aircraft have the CDR intent. They share individual intent throughout the simulation.

To confirm the robustness against the wind uncertainty, we performed five simulations under different wind speed vectors; that is, we applied five different z values to Eq. (17) within 2-sigma values. Figure 3 shows the simulated trajectories of the five simulations in these cases. In this figure, the blue, red, and green trajectories correspond to $i = 1$, 2, and 3, respectively, and the circles and arrows denote the target waypoints for individual aircraft and the travelling directions, respectively. As can be seen in the figure, we confirmed that the resulting trajectories were not sensitive to the wind uncertainty, because the proposed method directly optimizes the ground speed vectors rather than the airspeed vectors. The time histories of the intent parameters $r_k^{(i)}$ in one of the simulations in each case are shown in Fig. 4. The values of $r_k^{(i)}$ were kept at 0 for 20 s from the start of the simulation, because the intent inference was not activated during this period due to the lack of the number of time steps of the latest trajectories required for the intent inference. Except for the third aircraft in case B, the CDR intent was validated (i.e., $r_k^{(i)} = 1$) when four additional steps passed after

the initiation of the intent inference, that is, at $t = 28\,\mathrm{s}$, and both the CDR and WP intent were considered possible (i.e., $r_k^{(i)} = 0$) after the conflicts were resolved completely, though some oscillation of $r_k^{(1)}$ and $r_k^{(2)}$ between 0 and 1 was observed in case B. In contrast, $r_k^{(3)}$ in case B oscillated between 0 and -1 because the actual intent was WP. From the fact that the minimum separation in each simulation was approximately $R = 1{,}100\,\mathrm{m}$ (also see Fig. 6 below), and given the observations regarding Figs. 3 and 4, we can confirm that robust CDR without conservativeness was performed in each simulation by reflecting the validated or possible intent of individual aircraft.

Next, we considered CDR among six aircraft under the two cases defined above. In each case, we performed four simulations under different wind speed vectors. Figure 5 shows the trajectories of the four simulations in these cases. As can be seen in the figure, there were relatively large fluctuations in the trajectories, compared with the three-aircraft CDR problem. The minimum distance occurring in each simulation is shown in Fig. 6. It can be seen in this figure that the minimums in some simulations of the six-aircraft problem were slightly lower than $R = 1{,}100\,\mathrm{m}$. This was probably because of the delay to follow the calculated optimum of the ground speed vector. (Note that the optimization in the proposed method does not guarantee a separation distance greater than R when following the calculated optimum requires an actual delay. Thus, we set the value of R, including its margin, to take this effect into account.) Nevertheless, the minimum separation in each simulation was sufficiently close to $R = 1{,}100\,\mathrm{m}$, so we can confirm that robust CDR without excessive conservativeness was performed even in this problem.

Figure 7 shows the time histories of the actual airspeed magnitudes of all the simulations. Although the airspeed in small regions of some simulations was outside of the specified range (i.e., $[20\,\mathrm{m/s},\ 30\,\mathrm{m/s}]$), it was almost within the specified range as a whole due to the consideration of the wind uncertainty.

The computational time of the proposed method per sampling time was, in the worst case, less than $1.0\,\mathrm{s}$ using a common laptop computer and employing IBM® ILOG® CPLEX® 20.1.0 as the solver for the SOCP. Thus, for the tested simulations, the computational time was small enough compared to the sampling time step $\Delta t = 2.0\,\mathrm{s}$.

Table 1 – Parameters for simulations.

Parameter	Value	Parameter	Value
$V_{\min}^{(i)}, \forall i$	20 m/s	k_1	4
$V_{\max}^{(i)}, \forall i$	30 m/s	k_2	4
R	1,100 m	ε_1	0.8
Δt	2.0 s	ε_2	0.5
Inference steps	11	τ	4.0 s
γ	2.0		

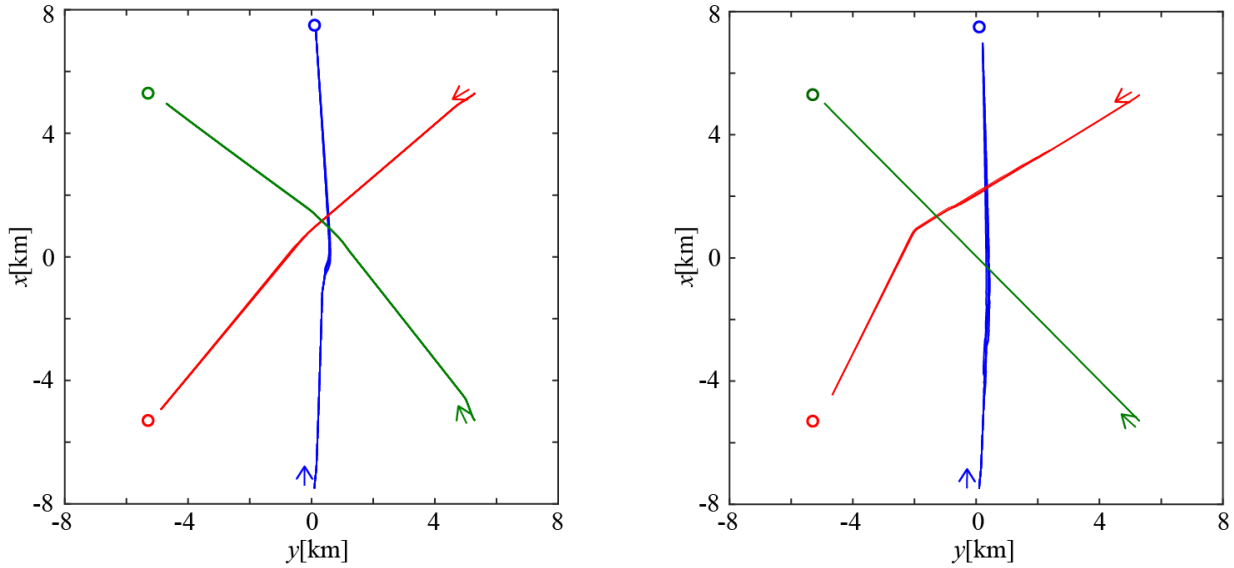

Figure 3 – Simulated trajectories of CDR among three aircraft in cases A (left) and B (right).

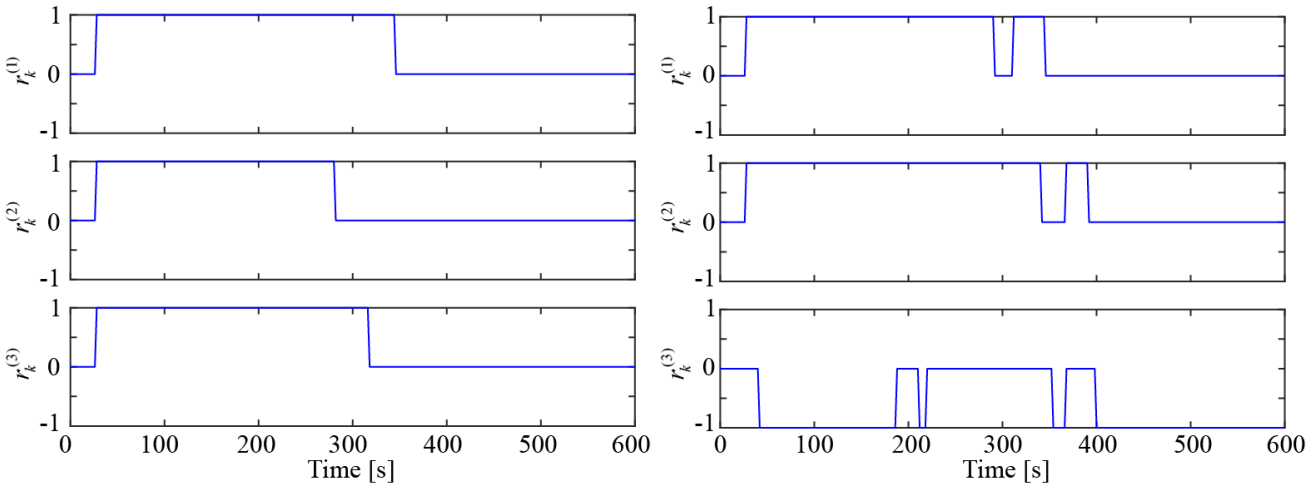

Figure 4 – Time histories of intent parameters $r_k^{(i)}$ in one simulation each for cases A (left) and B (right).

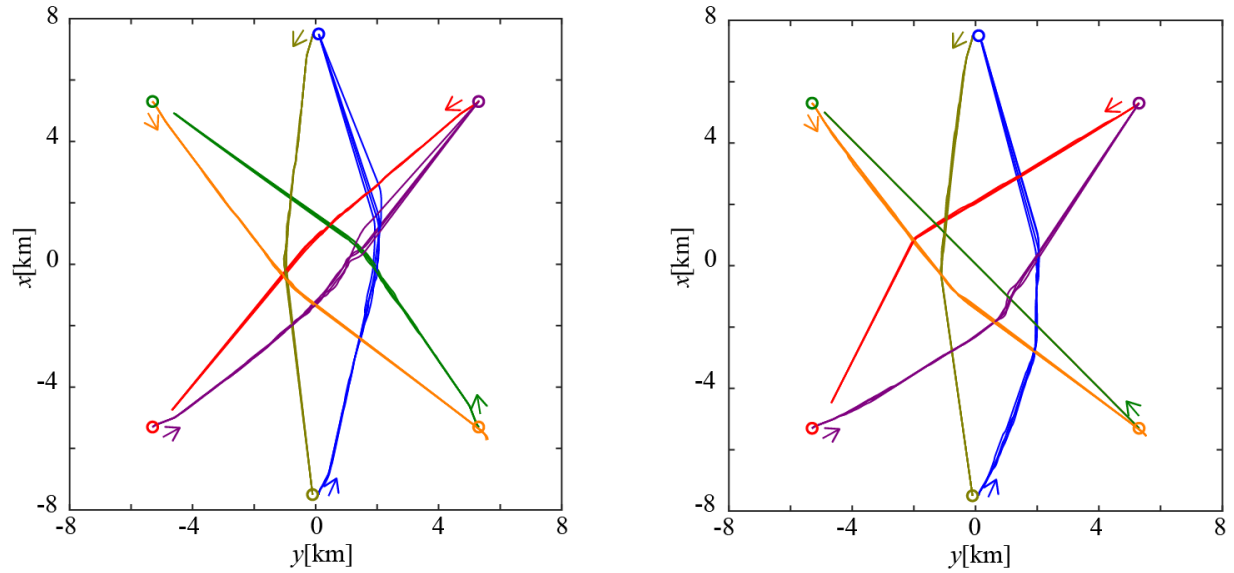

Figure 5 – Simulated CDR trajectories of six aircraft in cases A (left) and B (right).

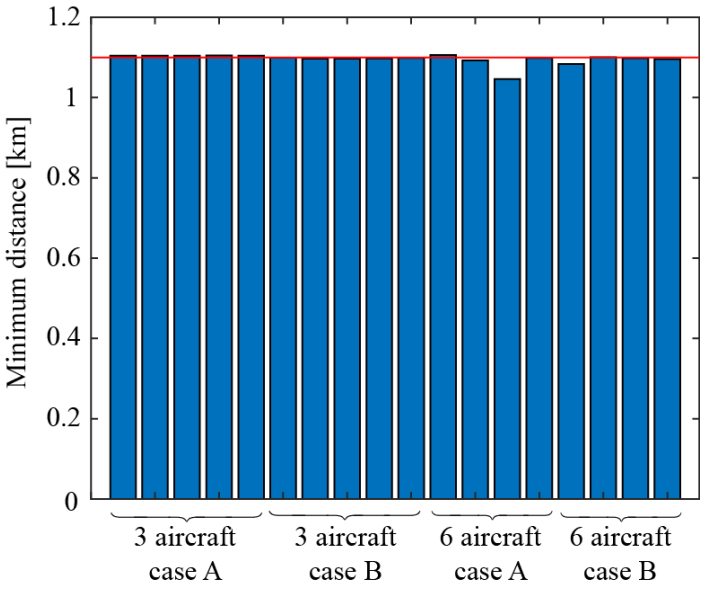

Figure 6 – Minimum distance occurring in each simulation. The horizontal red line marks R = 1,100 m.

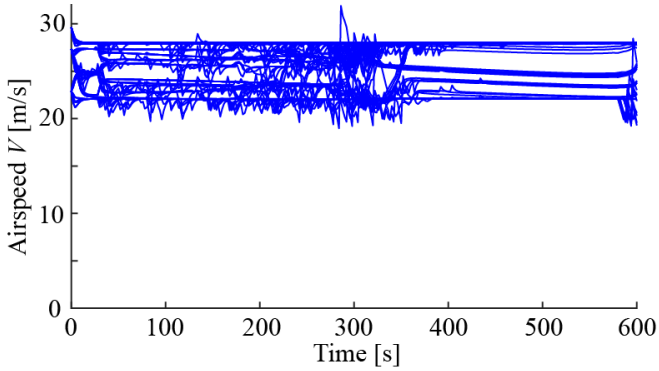

Figure 7 – Time histories of the airspeed magnitude for all the simulations.

4. Conclusions

In this paper, we propose a new method for the real-time CDR of multiple aircraft that accounts for the uncertainty of the flight intent of neighboring aircraft and the actual wind condition. Through numerical simulations, the effectiveness of the proposed method was demonstrated in terms of robustness and the reduced conservativeness of the calculated trajectories despite the uncertainty.

Future research will include, but is not limited to, extension of the proposed method to three-dimensional (i.e., horizontal and vertical) CDR, incorporation of a stochastic model predictive controller to robustly compensate for the future wind uncertainty, and further acceleration of the optimization algorithm for actual implementation.

5. Contact Author Email Address

yoko@nda.ac.jp

6. Copyright Statement

Acknowledgment

This research was supported by the Japan Society for the Promotion of Science, KAKENHI Grant Number JP18K04574.

References

[1] Ramasamy, S., Sabatini, R., Gardi, A. G. and Liu, Y., Novel flight management system for real-time 4-dimensional trajectory based operations, *Proceedings of AIAA Guidance, Navigation, and Control Conference*, AIAA 2013-4763, 2013

[2] Kuchar, J. and Yang, L., A review of conflict detection and resolution modeling methods," *IEEE Transactions on Intelligent Transportation Systems*, Vol. 1, No. 4, pp. 178-189, 2000.

[3] Krozel, J.,and, D. and Andrisani, D, Intent inference with path prediction, *Journal of Guidance, Control, and Dynamics*, Vol. 29, No. 2, pp. 225-236, 2006

[4] Yepes, J. L., Hwang, I. and Rotea, M., New algorithms for aircraft intent inference and trajectory optimization, *Journal of Guidance, Control, and Dynamics*, Vol. 30, No. 2, pp. 370-382, 2007

[5] Yokoyama, N., Inference of aircraft intent via Inverse optimal control including second-order optimality condition, *Journal of Guidance, Control, and Dynamics*, Vol. 41, No. 2, pp. 349-359, 2018

[6] Hwang I. and Seah, C. E., Intent-based probabilistic conflict detection for the next generation air transportation system, *Proceedings of the IEEE*, Vol. 96, No. 12, pp. 2040-2059, 2008

[7] Liu, W. and Hwang, I., Probabilistic trajectory prediction and conflict detection for air traffic control, *Journal of Guidance, Control, and Dynamics*, Vol. 34, No. 6, pp. 1779-1789, 2011

[8] Matsuno, Y., Tsuchiya, T., and Matayoshi, N., Near-optimal control for aircraft conflict resolution in the presence of uncertainty," *Journal of Guidance, Control, and Dynamics*, Vol. 39, No. 2, pp. 326-338 , 2016

[9] Yokoyama, N., Decentralized conflict detection and resolution using intent-based probabilistic trajectory prediction, *Proceedings of 2018 AIAA Guidance, Navigation and Control Conference (AIAA SciTech Forum)*, AIAA 2018-1857, 2018

[10]Frazzoli, E., Mao Z.-H., Oh, J.-H., and Feron, E., Resolution of conflicts involving many aircraft via semidefinite programming, Journal of Guidance, Control, and Dynamics, Vol. 24, No. 1, pp.79-86, 2001

[11]Yokoyama, N., Decentralized trajectory optimization of multiple aircraft using intent-based coordination, *Proceedings of 2018 AIAA Guidance, Navigation and Control Conference (AIAA SciTech Forum)*, AIAA 2021-0863, 2021

[12]Alizadeh, F. and Goldfarb, D., Second-order cone programming, *Mathematical Programming*, Ser. B, Vol. 95, pp.3-51, 2003

[13]Gill, P. E., Murray, W. and Margaret, H. W., *Practical Optimization*, Elsevier, Oxford, U.K., 1986, pp. 77-82.

[14]Huang, K. and Sidiropoulos, N. D., Consensus-ADMM for general quadratically constrained quadratic programming," *IEEE Transactions on Signal Processing*, Vol. 64, No. 20, pp. 5297 – 5310, 2016

[15]Horst, R. and Thoai N. V., DC programming: overview," *Journal of Optimization Theory and Applications*, Vol. 103, No. 1, pp. 1–43, 1999

[16]Lipp, T. and Boyd S., Variations and extension of the convex–concave procedure, Optimization and Engineering, Vol. 17, No. 2, pp. 263-287, 2016

[17]Yokoyama, N and Matsuno Y., Stochastic model predictive control for airspeed optimization using successive convexification, *Proceedings of 2019 AIAA Guidance, Navigation and Control Conference (AIAA SciTech Forum)*, AIAA 2019-1664, 2019